論文 7-1-5

"A Study on the Stress and Wave Propagation in Transversely Impacted Composite Laminates"

Kook-Chan Ahn* and Nam-Kyung Kim*

ABSTRACT

The impulsive stress and wave propagation of a glass/epoxy laminate subjected to the transverse low-velocity impact of a steel ball are investigated theoretically and experimentally. A plate finite element model based on Whitney and Pagano's theory in conjunction with experimental contact laws is used for the theoretical investigation.

The specimens for statical indentation and impact test are composed of $[0/45/0/-45/0]_{2s}$ and $[90/45/90/-45/90]_{2s}$ stacking sequences and have clamped-simply supported boundary conditions.

Finally, these two results are compared and then the impulsive stress and wave propagation characteristics of this laminated composite are studied.

요 약

강구에 의한 횡방향 저속 충격을 받게 되는 복합재의 충격 응력 및 파동 전파에 관한 이론적 및 실험적 연구가 행하여 진다. 이론적 해석을 위해서는 실험적 접촉 법칙과 연계된 Whitney와 Pagano의 이론에 근거한 판 유한 요소 모델이 사용되며, 실험적 해석을 위해서는 직접적인 충격실험이 수행된다.

이러한 해석을 위한 시험편은 $[0/45/0/-45/0]_{2s}$와 $[90/45/90/-45/90]_{2s}$ 적층 순서를 가지는 유리/에폭시 적층 복합재이며 경계 조건은 clamped-simply support이다.

결과적으로 이러한 두 해석 결과들이 비교 검토되며, 적층 복합재의 충격 응력 및 파동 전파 특성이 규명된다.

* Member : Chinju National Agricultural and Forestry Junior College, Dept. of Die and Mould Design

1. Introduction

The hard object impact usually gives a short contact time and results in the initial transmission of impact energy into a local region of the structure. This initial energy will propagate into the rest of the structure in the form of stress waves. Far field damage away from the impact area can result from the reflection of stress wave.

It is generally agreed that the cause of the sudden failure must be examined from the point of transient wave propagation phenomena.

The impulsive stress and wave propagation phenomena induced by impact loads in laminated composites are more complicated than those in homogeneous and isotropic plates due to the anisotropic and nonhomogeneous properties in the laminate.

A survey of wave propagation and impact in composite materials has been given by Moon[1]. Many analytical[2~3] and experimental[4~5] methods have been employed to study the wave propagation problems but many numerical[6~7] methods have not been used for these investigations.

In this study, the impulsive stresses and wave propagation characteristics of glass/epoxy laminates due to the transverse low-velocity impact of a steel ball are investigated theoretically and experimentally.

For theoretical investigation a dynamic finite element model based on Whitney and Pagano's theory[8] in conjunction with static contact laws by experiment is used and impact experiment using surface strain gages on the laminated plate is carried out for experimental investigation.

These two results are compared and then the impulsive stress and wave propagation phenomena of this laminated composite are studied.

2. Theoretical formulation

Consider a plate of uniform thickness h composed of a finite number of anisotropic layers with arbitrary orientations. The coordinate system is chosen such that the middle plane, R, of the plate coincides with the x-y plane with z-axis normal to the middle plane.

The displacement field in the shear deformable theory of Whitney and Pagano[8] is given by

$$\begin{aligned} u(x,y,z,t) &= u^0(x,y,t) - z\phi_x(x,y,t) \\ v(x,y,z,t) &= v^0(x,y,t) - z\phi_y(x,y,t) \\ w(x,y,z,t) &= w^0(x,y,t) \end{aligned} \tag{1}$$

where u, v and w are the displacements along x, y and z directions respectively, u^0 and v^0 are the in-plane displacements of the middle plane, ϕ_x and ϕ_y are the shear rotations, and t is the time.

The stress-strain relations of k-th lamina in laminate reference axes(x, y, z) is

$$\begin{Bmatrix} \sigma_{xx} \\ \sigma_{yy} \\ \sigma_{xy} \\ \sigma_{yz} \\ \sigma_{zx} \end{Bmatrix}^k = \begin{bmatrix} \bar{Q}_{11} & \bar{Q}_{12} & \bar{Q}_{16} & 0 & 0 \\ \bar{Q}_{12} & \bar{Q}_{22} & \bar{Q}_{26} & 0 & 0 \\ \bar{Q}_{16} & \bar{Q}_{26} & \bar{Q}_{66} & 0 & 0 \\ 0 & 0 & 0 & \bar{Q}_{66} & \bar{Q}_{45} \\ 0 & 0 & 0 & \bar{Q}_{45} & \bar{Q}_{55} \end{bmatrix}^k \begin{Bmatrix} \varepsilon_{xx} \\ \varepsilon_{yy} \\ \gamma_{xy} \\ \gamma_{yz} \\ \gamma_{zx} \end{Bmatrix}^k \tag{2}$$

where

$$\{\varepsilon\}^k = \begin{Bmatrix} \varepsilon_{xx} \\ \varepsilon_{yy} \\ \gamma_{xy} \\ \gamma_{yz} \\ \gamma_{zx} \end{Bmatrix}^k = \begin{Bmatrix} \varepsilon^0 \\ 0 \end{Bmatrix} + \begin{Bmatrix} Zk \\ \gamma^0{}_z \end{Bmatrix}$$

$$\{\varepsilon^0\} = \begin{Bmatrix} u^0,\ x \\ v^0,\ y \\ u^0,y+v^0,x \end{Bmatrix}, \quad \{k\} = \begin{Bmatrix} -\phi_{x,y} \\ -\phi_{y,y} \\ -(\phi_{x,y}+\phi_{y,u}x) \end{Bmatrix}$$

$$\{\gamma^0{}_z\} = \begin{Bmatrix} w,y-\phi_y \\ w,x-\phi_x \end{Bmatrix} \tag{3}$$

in which σ_{ij} are stresses, ε_{ij} and γ_{ij} are strains, and $\bar{Q}_{ij}$ are the material coefficients in the plate coordinates.

Assuming monoclinic behavior(i.e., existence of one plane of elastic symmetry) for each layer, the constitutive equations for an arbitrarily laminated plate are

$$\begin{Bmatrix} N \\ M \\ Q \end{Bmatrix} = \begin{bmatrix} A & B & 0 \\ B & D & 0 \\ 0 & 0 & H \end{bmatrix} \begin{Bmatrix} \varepsilon^0 \\ K \\ \gamma^0 z \end{Bmatrix} \tag{4}$$

by

$$(A_{ij},\ B_{ij},\ D_{ij}) = \int_{-h/2}^{h/2} \bar{Q}_{ij}(1, z, z^2)dz \quad (i,j=1,2,6)$$
$$(H_{ij}) = \int_{-h/2}^{h/2} k_i k_j \bar{Q}_{ij} dz \quad (i,j=4,5) \tag{5}$$

where k_i are the shear correction coefficients.

The equilibrium equations are given by

$$\begin{aligned} &N_{x,x} + N_{xy,y} = P\ddot{u} + R\ddot{\phi}_x \\ &N_{xy,x} + N_{xy,y} = P\ddot{v}_y + R\ddot{\phi}_y \\ &M_{x,x} + M_y - Q_x = R\ddot{u}^0 + I\ddot{\phi}_x \\ &M_{xy,x} + M_{y,y} - Q_y = R\ddot{v}^0 + I\ddot{\phi}_y \\ &Q_{x,x} + Q_{y,y} + q = P\ddot{w}^0 \end{aligned} \tag{6}$$

where P, R and I are the normal, coupled normal-rotary and rotaty inertia coefficients,

$$(P, R, I) = \int_{-h/2}^{h/2} \rho^{(m)}(1, z, z^2)dz \tag{7.a}$$

$\rho^{(m)}$ being the material density of the m-th layer.

In equation(6), q is the transversely distributed force, and N_i, Q_i and M_i are the stress and moment resultants defined by

$$(N_x, N_y, N_{xy}) = \int_{-h/2}^{h/2} (\sigma_x, \sigma_y, \sigma_{xy})dz$$
$$(M_x, M_y, M_{xy}) = \int_{-h/2}^{h/2} (\sigma_x, \sigma_y, \sigma_{xy})dz \tag{7.b}$$
$$(Q_x, Q_y) = \int_{-h/2}^{h/2} (\sigma_{zx}, \sigma_{yz})dz$$

Following the standard finite element procedure using above equations, we obtain the equations of motion of the impactor-plate system

$$\begin{aligned} F &= -m_s \ddot{w}_s = -k\alpha^n \quad \text{(for loading process)} \\ &= F_m \left[\frac{\alpha - \alpha_0}{\alpha_m - \alpha_0}\right]^q \quad \text{(for unloading process)} \end{aligned} \tag{8}$$

and

$$[M]\{\ddot{\Delta}\} + [K]\{\Delta\} = \{F\} \tag{9}$$

where m_s is the mass of impactor, k is the coefficient, F_m is the maximum contact force, α_m is the contact indentation in F_m, α_0 is the permanent indentation, [M] is the mass matrix, [K] is the linear elastic stiffness matrix and {F} is the contact force vector.

The contact force F between the plate and impactor is calculated by equation(8) and must be calculated before the equation(9) can be analyzed.

In this equation(8), indentation α is given by

$$\alpha = w_s(t+\Delta t) - w(x_0, y_0, t+\Delta t) \tag{10}$$

in which w and w_s is the plate and impactor deflection at the impact point (x_0, y_0), respectively. (Fig. 1)

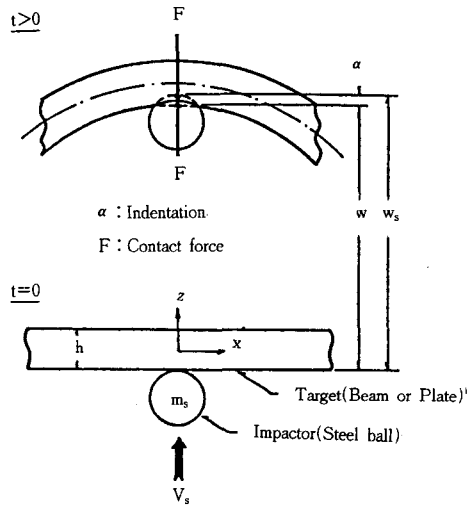

Fig. 1 Cental transverse impact of a rigid body

The finite element model used here is a four-node isoparametric quadrilateral element. Five degrees of freedom, i.e.,

$\{\Delta\} = [u_i,\ v_i,\ w_i,\ \phi x_i,\ \phi y_i]^T$, are assumed at each node.

In the numerical integration of the stiffness[K], the so-called reduced integration method is employed. The 2×2 Gaussian rule is used to compute the stiffness coefficients for the in-plane and bending deformation, and the reduced 1×1 Gaussian rule to compute the stiffness coefficients for transverse shear deformation.

The solution for the equations for motion given by equation(8) and (9) can be solved by time integration

algorithm developed by Wilson and Clough[9].

3. Experiment

3-1. Specimens

Stacking sequences of the specimens for static indentation and impact test were $[0/45/0/-45/0]_s$ and $[90/45/90/-45/90]_{2s}$, and dimensions were $4.5^t \times 200^w \times 200^l$(mm) and $4.5^t \times 300^w \times 300^l$(mm).

In all tests, the specimens had clamped-simply supported boundary conditions.

For material properties of the specimens, the tensile tests using specimens by ASTM rule were carried out. These results were shown in Table 1.

Table 1 Material properties of the specimen and steel ball

Material properties	E_1	E_2	G_{12}	ν_{12}	ρ
	GPa			−	Kg/m^3
Specimen	55.85	14.75	6.43	0.31	2050
Steel ball	207		79.6	0.30	7860

3-2. Static indentation test

The experimental setup is shown in Fig. 2. The dial gage was mounted on a "ㄷ" bracket fixed to the loading piston so that only the relative displacement between the indentor and the specimens was recorded.

The load was applied by Universal Test Machine (UTM25T) in loading and unloading processes and X-Y plotter was used to obtain continuous force-indentation curves. A spherical steel indentor of diameter 12.7mm was used.

These experimental static contact laws for loading and unloading processes are used for a dynamic finite element analysis.

3-3. Impact test

The experimental setup is shown in Fig. 3. The strain responses at three points on the plate were measured by means of surface strain gages.

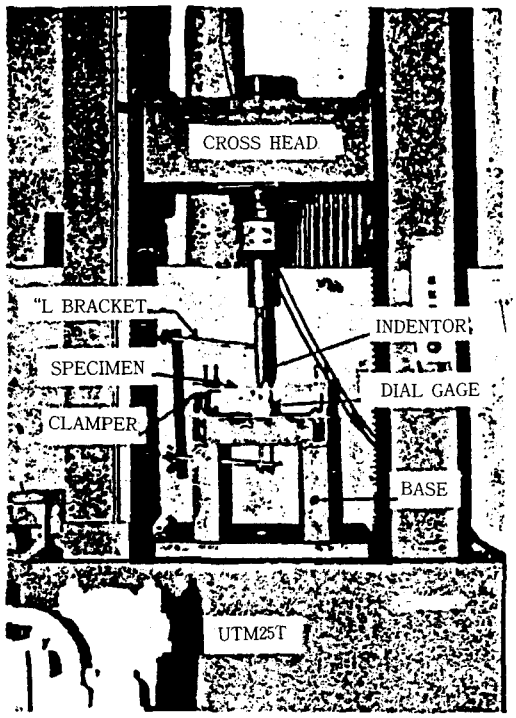

Fig. 2 Equipment for static test

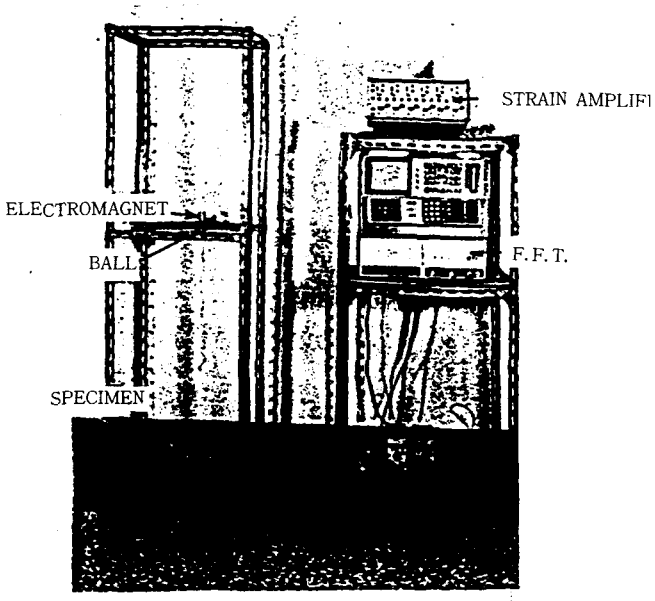

Fig. 3 Equipment for impact test

Three strain gages(KYOWA Electronic Instruments Co., TYPE KFC-2-D17-11) were placed at different locations as shown in Fig. 4 to record the dynamic strain histories. Impact velocity is 4m/sec. and diameter of impactor is 12.7mm. Signals from gages were amplified by a dynamic strain amplifier and recorded at the F.F.T..

(Units : mm)

Model	Measuring points		
Length		L=200	L=300
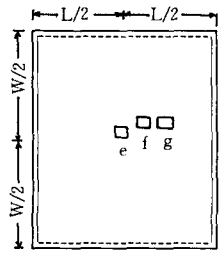 (h : plate thickness)	e	(x, y, z)=(0.0, 0.0, h/2)	(x, y, z)=(3.2, 3.2, h/2)
	f	(2.1, 2.1, h/2)	(3.2, 3.2, h/2)
	g	(44.2, 2.1, h/2)	(66.3, 3.2, h/2)
	Note : Strain gages at measuring points a and e are located for trigger of impact responses. *Boundary conditions* ; —— : clamped ----- : simply-supported		

Fig. 4 Measuring points according to the change of model type

4. Results and discussion

The contact laws for the 12.7mm steel indentor and glass/epoxy laminate were determined experimentally by means of a statical indentation test.

The plate specimens were clamped-simply supported at four ends. Loading and unloading curves were fitted into power equations by least square method and their results were shown in Fig. 5.

The statically determined contact laws were incorporated into an developed four-node isoparametric plate finite element program to obtain the impact response of glass/epoxy laminated plate due to impact.

An impact experiment was conducted on a glass/epoxy laminated plate to verify the validity of the dynamic finite element analysis. The strain responses predicted using the finite element method agreed very well with the test results as shown in Fig. 6~Fig. 7.

Through these theoretical and experimental strain(stress) responses, we could predict the impulsive strain(stress) and wave propagation characteristics in glass/epoxy lamin-

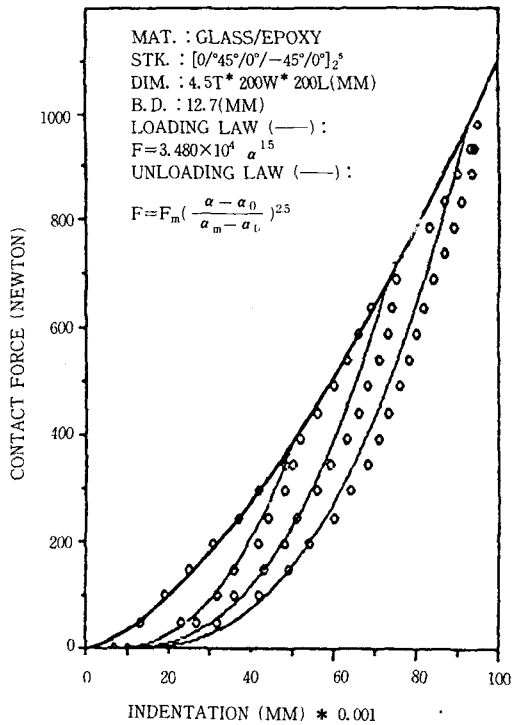

Fig. 5 Loading and unloading curves for $[0°/45°/0°/-45°/0°]_{2s}$ glass/epoxy plate with 200mm length

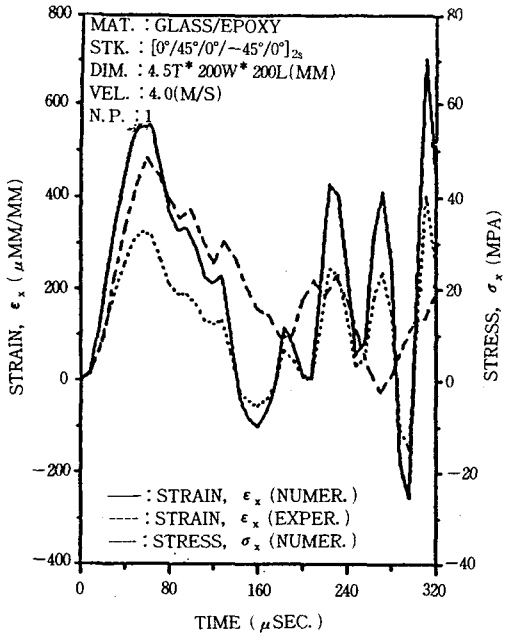

Fig. 6 Strain and stress response histories for a $[0°/45°/0°/-45°/0°]_{2s}$ glass/epoxy plate at 2.1mm from the impact point

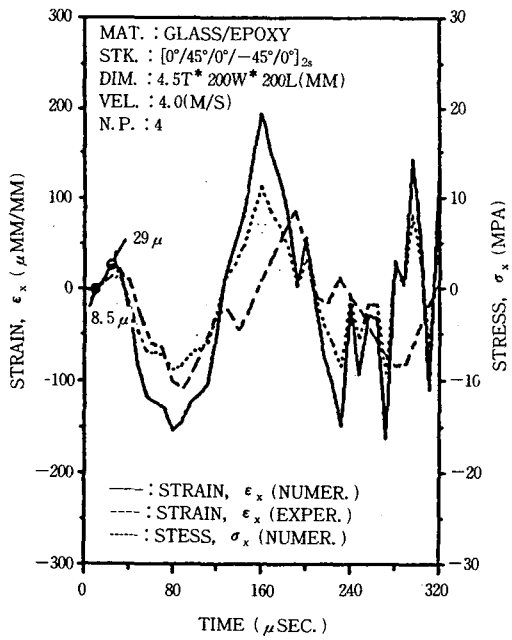

Fig. 7 Strain and stress response histories for a $[0°/45°/0°/-45°/0°]_{2s}$ glass/epoxy plate at 44.2mm from the impact point

Table 2 Comparison of maximum value from each point by numerical simulation

Material	Specimen dimension	Notation		At 44.2(66.3*)mm from impact point		At 2.1(3.2*)mm from impact point	
	w×l(mm)	Strain	Stress	Value		Value	
				μmm/mm	MPa	μmm/mm	MPa
Glass/epoxy	200×200	ε_x^0	σ_x^0	−155	−8.9	567	32.5
		ε_x^{90}	σ_x^{90}	−198	−3.0	800	12.1
		ε_y^0	σ_y^0	—	—	804	14.8
		ε_y^{90}	σ_y^{90}	—	—	570	36.4
	300×300*	ε_x^0	σ_x^0	−87	−5.0	402	23.1
		ε_x^{90}	σ_x^{90}	−112	−1.7	543	8.2
		ε_y^0	σ_y^0	—	—	539	10.0
		ε_y^{90}	σ_y^{90}	—	—	402	25.6

Superscripts { 0 : top part of $[0°/45°/0°/-45°/0°]_{2s}$ laminate
90 : top part of $[90°/45°/90°/-45°/90°]_{2s}$ laminate

Table 3 Comparison of wave velocity from numerical simulation and impact experiment

Material	Specimen dimension	Wave propagation theory		Numerical simulation	Impact experiment
	w×l(mm)	Wave type	Wave velocity(m/sec.)		
			At all points	At 44.2(66.3*)mm from impact point	
Glass/epoxy	200×200	C_L^0	5286	5200	4911
		C_L^{90}	2716	3844	3536
		C_F^0	1771	1524	1450
		C_F^{90}		1263	1163
	300×300*	C_L^0	5286	4736	4420
		C_L^{90}	2716	3400	3234
		C_F^0	1771	1411	1326
		C_F^{90}		1228	1153

Superscripts: 0 : top part of $[0°/45°/0°/-45°/0°]_{2s}$ laminate; 90 : top part of $[90°/45°/90°/-45°/90°]_{2s}$ laminate

Subscripts: L : longitudinal wave(in-plane wave); F : flexural wave(transverse wave)

ated composite as shown in Table 2 and Table 3.

5. Conclusions

Through the theoretical and experimental impact responses, we obtained the following conclusions;

(1) In general, theoretical in-plane and leading flexural wave velocities agreed well with the corresponding values by experiment.

(2) The predominent wave induced by central impact has found to be a flexural one propagating at different velocities in different directions.

(3) The flexural wave velocity is higher in the higher modulus direction and the amplitude of the flexural wave is much larger than that of the in-plane wave.

(4) Appreciable modulus and strength degradation may be produced due to large strain(stress) in the neighborhood of the impact point and in special, large strain in the transverse to the fiber direction.

REFERNCES

1) Moon, F.C., NASA CR-121226, 1973.

2) Sun, C.T., Journal of Composite Materials, Vol.7, 1973, pp.366~382.

3) Moon, F.C., Journal of Composite Materials, Vol.6, 1972, pp.62~76.

4) Takeda, N., Sierakowski, R.L. and Malvern, L.E, Journal of Composite Materials, Vol.15, 1981, pp.157~174.

5) Hayashi, T., Ugo, R. and Morimoto, Y., Experimental Mechanics, June 1986, pp.169~174.

6) K.C. Ahn, M.S. Kim and G.N. Kim, Trans. KSME, Vol.12, No.4, 1988, pp.652~661.

7) K.C. Ahn, M.S. Kim and G.N. Kim, Trans. KSME, Vol.13, No.1, 1989, pp.9~19.

8) Whitney, J.M. and Pagano, N.J., Journal of Applied Mechanics, Vol.37, 1970, pp.1031~1036.

9) Wilson, E.L. and Clough, R.W., Symp. on Use of Computers in Civil Engng.